Available online at www.sciencedirect.com
SCIENCE DIRECT
ELSEVIER
Palaeogeography, Palaeoclimatology, Palaeoecology 237 (2006) 240–254
PALAEO
www.elsevier.com/locate/palaeo

Paleoenvironmental record in Lake Baikal sediments: Environmental changes in the last 160 ky

T. Grygar [a,*], J. Kadlec [b], P. Pruner [b], G. Swann [c], P. Bezdička [a], D. Hradil [a], K. Lang [a], K. Novotna [a], H. Oberhänsli [d]

[a] *Institute of Inorganic Chemistry AS CR, 250 68 Rez, Czech Republic*
[b] *Institute of Geology AS CR, Rozvojova 135, 165 02 Praha 6, Czech Republic*
[c] *Department of Geography, University College London, 26 Bedford Way, London WC1H 0AP, UK*
[d] *GeoForschungsZentrum, Potsdam, D-14473 Potsdam, Germany*

Received 17 August 2005; received in revised form 22 November 2005; accepted 5 December 2005

Abstract

Measurement of magnetic susceptibility (MS) and diffuse reflectance spectra (DRS) were used to construct environmental proxies in a 6.5 m section of the sediment core VER98-1-13 from the Academician Ridge, Lake Baikal. The interpretation of MS and DRS was supported by X-ray diffraction and microparticle voltammetry to identify the main Fe-bearing minerals. The record of the relative paleointensity of the Earth's magnetic field was used to construct an age model showing the core interval covers the last 160 ky. The time resolution of the record was ~1 ky. The main environmental changes were recognized by a combination of DRS and MS records and compared to marine isotopic stages in addition to the diatom record from 120 to 60 ky BP so as to demonstrate the importance of these inorganic proxies as paleoenvironmental records. A dramatic climatic deterioration between 66 and 60 ky BP was probably preceded by a dry intermediate stage between 77 and 66 ky BP. The DRS-based proxies of Fe(II)/Fe(III) ratios in the mineral assemblage, MS and/or diatom records clearly reveal 1–2 ky long environmental extremes at 110, 103, 90, 85, 77, 61, 54, 36, 27, 23, and 19 ky BP. The majority of these extremes were contemporaneous with discharges of North Atlantic and Arctic Ocean icebergs (Heinrich events) documenting a teleconnection between the North Atlantic Ocean and East Central Siberia. These sharp changes coincided with a major transition to the colder climatic stages of the last 100 ky.

Keywords: Lake sediments; Climate change; Spectroscopy; Magnetic methods

1. Introduction

Lake Baikal's sediments are one of the most valuable terrestrial climatic archives covering the last 20 My (Kashiwaya, 2003). In certain Baikal localities, particularly those close to the deltas of the Selenga and Barguzin rivers, erosional and reworking events can be recognized in the influx of river-transported material (Prokopenko et al., 2001a). Contrarily on ridges relatively remote from the large river deltas (Academician Ridge, Continent Ridge) very fine and uniform material is deposited and sedimentation proceeded continuously, mostly without hiatuses, during the last hundred ky to several My with low and surprisingly stable sedimentation rate (Grachev et al., 1998; Bangs et al., 2000; Prokopenko et al., 2001b; Kravchinsky et al., 2003;

* Corresponding author. Fax: +49 420 220941223.
E-mail address: grygar@iic.cas.cz (T. Grygar).

0031-0182/$ - see front matter © 2006 Published by Elsevier B.V.
doi:10.1016/j.palaeo.2005.12.007

Demory et al., 2005a). In previous studies, the Baikal climatic record was mostly interpreted using explicit functions of the lake paleoproductivity such as diatom analysis (Edlund and Stoermer, 2000; Mackay et al., 2003; Roiual and Mackay, 2005; Swann et al., 2005), total content of biogenic SiO_2 (Bradbury et al., 1994; Prokopenko et al., 2001b; Ryves et al., 2003; Chebykin et al., 2004), pollen (Granoszewski et al., 2005) and the total organic carbon or C- and N-isotopic signatures (Prokopenko and Williams, 2003; Watanabe et al., 2003). Climatic variations, though, also affect sediment magnetic susceptibility (Peck et al., 1994; Demory et al., 2005a), which is implicitly related to the lake's bioproductivity by the dilution and/or reductive dissolution of ferrimagnetic particles. As such, this connection documents that a composition of Fe minerals in the sediment bears a paleoclimatic record.

Diffuse Reflectance Spectroscopy (DRS) is a convenient method allowing the identification of Fe-bearing minerals in marine or terrestrial sedimentary series, soils, and loess. DRS has been used to analyze climatically forced changes in the source areas of Quaternary marine sediments (Balsam et al., 1995; Cortijo et al., 1995; Helmke et al., 2002; Balsam and Beeson, 2003). The straightforward interpretation of the spectra is based on the evaluation of the reflectivity (darkness or lightness) which is related to the total content of white component strongly scattering light such as $CaCO_3$ (Cortijo et al., 1995; Helmke et al., 2002). Further quantitative information can be obtained by the recognition of the main coloring components using color indices (Helmke et al., 2002) or the first derivative of the reflectance spectra (Deaton and Balsam, 1991; Balsam et al., 1995; Balsam and Beeson, 2003). These approaches are very efficient if a white matrix contains one or several well-defined coloring agents with the compounds of fixed spectral properties directly related to sediment source area (Balsam and Beeson, 2003). A different approach is based on the deconvolution of the absorption spectra to distinct absorption bands (Grygar et al., 2003; Hradil et al., 2004) which are assigned to individual electron transitions of Fe ions in a specific structural environment. This approach is ideal if the number and kind of coloring agents are not known, as occurs in Lake Baikal's sediments which contains numerous colored minerals such as amphiboles, Fe-bearing micas, chlorites, and expandable clay minerals (Grachev et al., 1998; Horiuchi et al., 2000; Fagel et al., 2003; Grygar et al., 2005).

The most important recent achievements in the study of the Upper Pleistocene and Holocene sediments in Lake Baikal are the development of age models independent of the marine $\delta^{18}O$ record. These involve stacking numerous sedimentary series from different parts of the lake (Academician Ridge, Continent Ridge, Buguldeika Saddle and the Selenga delta), and systematically comparing the biogenic, chemical, magnetic and mineralogical proxies. In a series of recent studies independent age models were also developed based on radiocarbon dating (Prokopenko et al., 2001a,b), U/Th dating (Chebykin et al., 2004; Goldberg et al., 2005), and the relative paleointensity of magnetic fields (Pruner et al., 2004; Demory et al., 2005a,b). This offers a chance to search for possible discrepancies (lags and leads) in the timing of climatic changes in marine and terrestrial environments which was not possible in previous studies where secondary age models were derived from Milankovitch cycles or through correlation to SPECMAP.

The aim of this study is to identify the main environmental stages in the Lake Baikal watershed using mineralogical proxies based on Fe speciation by DRS, MS, and voltammetry of microparticles. These methods provide information about Fe oxidation state and the composition of Fe-bearing minerals. Further rock-magnetic methods and powder X-ray diffraction were also used in the study with diatom analysis between 120 and 60 ky BP done to aid comparison and paleoenvironmental interpretation of the inorganic proxies. The sediment series was obtained from the gravity and Kullenberg cores VER98-1-13 from the western part of the Academician Ridge, Lake Baikal, in 1998. Previous clay mineral analysis has indicated an environmentally controlled change in the sediment source area during the last glacial cycle (Grygar et al., 2005). In this study we focus on a period corresponding approximately to Marine Isotopic Stages (MIS) 5, 4, 3, and 2 which has previously only been rarely addressed in this area. Sediments from the Academician Ridge have previously been described in several studies Grachev et al., 1998; Horiuchi et al., 2000; Prokopenko et al., 2001b; Kravchinsky et al., 2003; Chebykin et al., 2004; Grygar et al., 2005) but none have focused on Fe speciation nor used DRS. The age model in this study was constructed from variation in the paleointensity of the Earth's magnetic field following the approach previously used elsewhere by Demory et al. (2005a).

2. Materials and methods

Samples were obtained from pilot and piston cores VER98-1-13 with a composite length of about 12 m from the Academician Ridge (Latitude 53.561°N, Longitude 108.011°E) at a water depth of 335 m (Fig. 1).

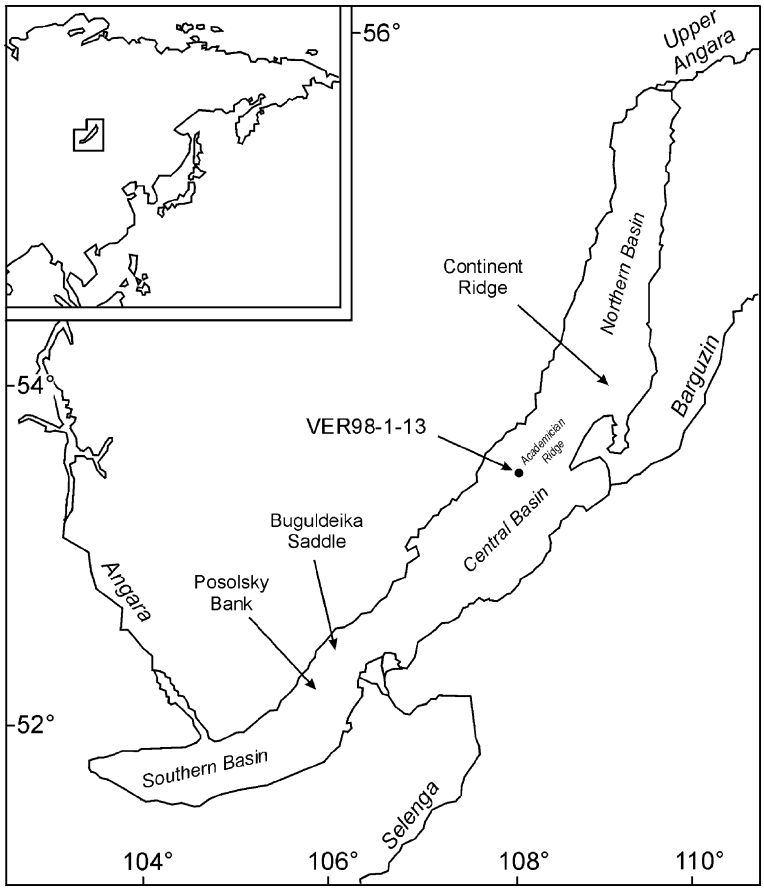

Fig. 1. Map of Lake Baikal with the most frequently studied localities. VER98-1-13 core is indicated by a circle.

The core was stored in a sealed Al tube at 4 °C. After opening the core the sediment appearance was examined and the material was sampled for magnetic measurements. The pilot and piston cores, which partially overlapped, were combined by matching their magnetic susceptibility records. Only the upper section of the resulting series was studied with, according to the age model, the composite length of 6.5 m covering the last 160 ky. Clay minerals have previously been analyzed on this core (Grygar et al., 2005).

2.1. Magnetic measurements and age model

Magnetic susceptibility was obtained after sampling the core using plastic cubes with an inner volume of 7 cm^3 and a mean vertical distance of 2.2 cm. Low field magnetic volume susceptibility (MS) was measured with a Kappabridge KLY-3S (sensitivity of $1.2 \cdot 10^{-8}$ SI). The samples were measured in a wet state as they were removed from the cores. Remanent magnetization (RM) was obtained with JR-6A or JR-5A spinner magnetometers. All samples were demagnetized in alternating fields with an amplitude 20 mT by an LDA-3A device to remove viscous overprints; the value so obtained was denoted RM20. Anhysteretic remanent magnetization (ARM), a measure of a total concentration of magnetic minerals, was generated along the sample positive z-axis with 0.05 mT static field parallel to the AF demagnetizing field on an AMU-1A device; the value of ARM20 was obtained after 20 mT alternating field demagnetization. The relative paleointensity of the magnetic field was estimated as quotient RM20/ARM20.

2.2. Analytical methods

Diffuse reflectance spectra were obtained using a Perkin Elmer Lambda 35 spectrometer equipped with an integrating sphere (Labsphere). For this, subsamples from the magnetic measurements were dried at 50 °C and ground in an agate mortar. The spectra of these powders was measured in 10 mm quartz cells between 250–1100 nm (40000–9090 cm^{-1}) with a 0.5 nm step. The reflectance was converted to the Kubelka–Munk scale, and processed using OriginPro7.0 software (Ori-

ginLab Co., USA). The spectral deconvolution was performed after smoothing the spectra by a 25-point Fourier filter and fitted by a set of Gaussian curves as described in Grygar et al. (2003) and Hradil et al. (2004). The deconvolution was performed with seven Gaussian bands, denoted hereafter by capital letters A–G, with the bandwidths refined with certain restrictions (sharing and/or upper limit setting to 3000 cm^{-1}). The bands were assigned according to Sherman (1985, 1987), Barrón and Torrent (1986), Deaton and Balsam (1991), and Hradil et al. (2004). The spectra of goethite pigment Bayferrox 3920 (Bayer, Germany) diluted to 3% by kaolinite white was used for comparison.

Voltammetry of microparticles was performed with a conventional paraffin impregnated graphite electrode in a 1 : 1 acetate buffer with a total acetate concentration of 0.2 M (Grygar et al., 2002, 2003; Grygar and van Oorschot, 2002). The peak potentials E_P were related to a saturated calomel reference electrode (SCE). The voltammograms were obtained by linear scans from open-circuit potentials toward −1.05 V vs. SCE to identify $Mn^{III,IV}$ and Fe^{III} oxides or to +1.0 V vs. SCE to identify Fe sulfides. The electrochemically active species were assigned by comparing their E_P with those of the reference compounds: Fe^{III} oxides (Grygar et al., 2002, 2003; Grygar and van Oorschot, 2002), $Mn^{III,IV}$ oxides (Bakardjieva et al., 2000) and Fe sulfides (Almeida and Giannetti, 2003).

Powder X-ray diffraction (XRD) of the dried samples was performed with a diffractometer PANalytical X'Pert PRO (CoKα radiation, linear detector X'Celerator) to obtain a common identification of the mineral constituents.

Samples for diatom taxonomy were prepared using a protocol that omits any chemical treatments or centrifugation in order to minimise further diatom dissolution and valve breakage (Mackay et al. 1998. Diatom concentrations were calculated by adding a well-defined amount of divinylbenzene microspheres, a method detailed by Battarbee and Kneen (1982). Diatom valves were counted under light microscope using phase contrast with an oil immersion lens at ×1000 magnification. Where possible 300 diatom valves were counted and classified per slide. In some samples the scarcity of preserved diatoms within the sedimentary record prevented this. Similar problems during periods of lower productivity in Lake Baikal have previously been experienced by Edlund and Stoermer (2000) and Swann et al. (2005). In such instances a minimum of 100 diatom valves or four transects were counted per slide.

3. Results

3.1. Core description and the age model

Sediment lithology (Fig. 2) indicated that the upper part of the core with its diatomaceous layer included the

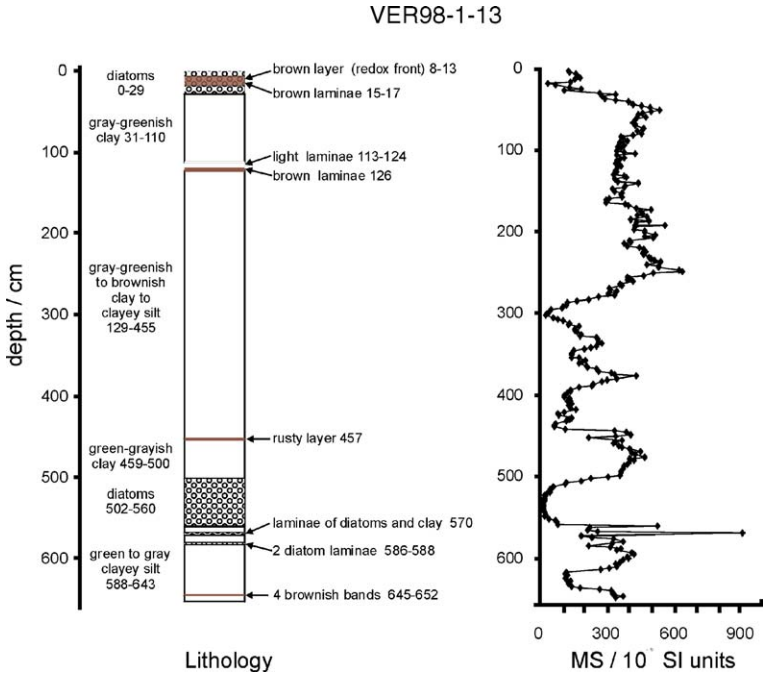

Fig. 2. Description of the VER98-1-13 core. Left: lithology, right: MS record.

Holocene. The second main diatom zone between 5.0 and 5.6 m corresponds to the Kazantsevo interglacial, the warmest interval of MIS 5 in Eurasia (Grachev et al., 1998). The main boundaries between major climatic stages can be easily revealed from the magnetic susceptibility (MS) record (Fig. 2). MS decreases in warmer periods (Peck et al., 1994) that is explained by a reductive diagenesis with a possible contribution from the dilution of detrital magnetite by diatom frustules (Peck et al., 1994; Demory et al., 2005b). Termination II (the transition between MIS 6 and MIS 5) was recognized by a change from clayey material to diatomaceous mud at 5.6 m. Between 5.6 and 2.8 m the MS pattern has several minima, corresponding to the warmer substages of the last interglacial, and a well-defined maximum corresponding to the cold period MIS 5d between 5.0 and 4.4 m.

The preliminary age model for the core was based on the comparison of the magnetic susceptibility record with a benthic foraminifera oxygen isotope curve from a North Atlantic reference core (Grygar et al., 2005). To obtain a more precise age model we used the method of Nowaczyk and Antonow (1997) based on the variations of the relative paleointensity in the Earth magnetic field (Fig. 3). Good correlation between such paleointensity records obtained in Baikal sediments and reference records from ODP984 and Sint-800 has recently been confirmed by Oda et al. (2002). As a reference we selected the record from ODP Site 984 (Channell, 1999). In the upper 5.5 m of the sediment 37 tie points were chosen by comparing local paleointensity minima and maxima from the two cores. For clarity, only the local minima are connected by lines,

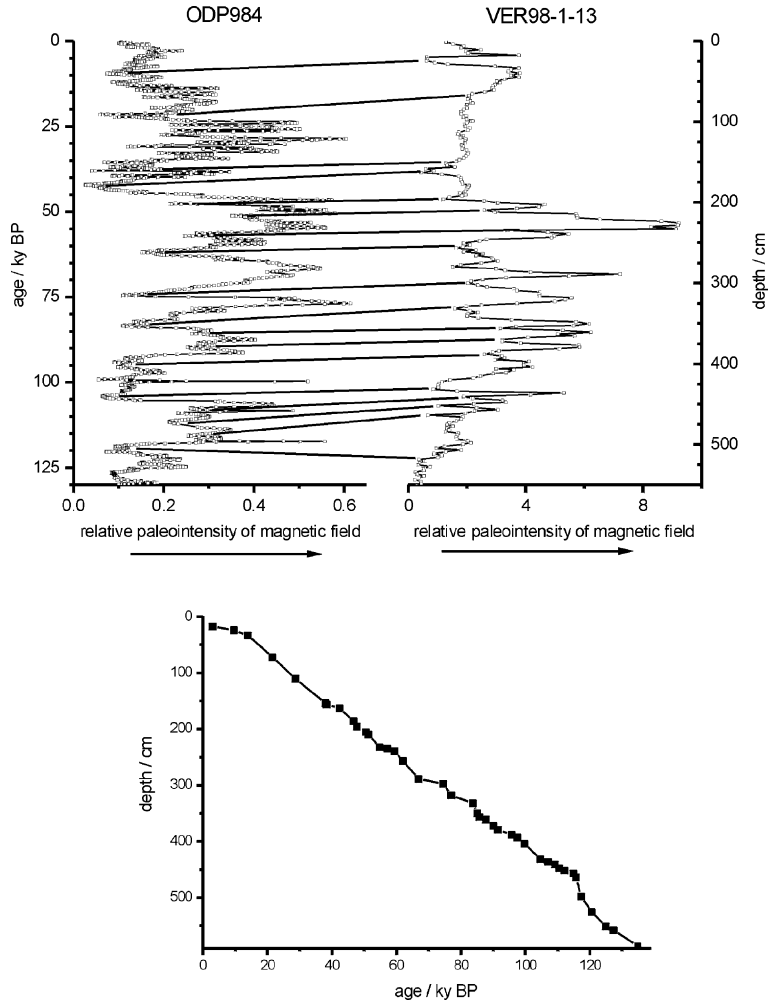

Fig. 3. The age model based on the comparison of the relative paleointensity of the Earth's magnetic field. Top: the relative paleointensity of the reference core (top left, ODP984, Channell, 1999) and in VER98-1-13 (top, right). Half of the tie points (the lines connecting paleointensity minima) are shown. Bottom: The age versus depth model for VER98-1-13, all tie points are shown.

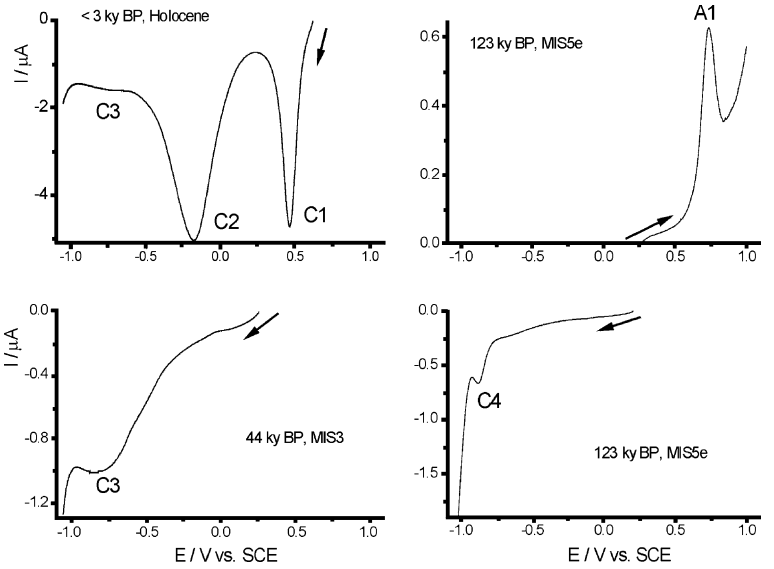

Fig. 4. Voltammograms of the brownish bands in the redox front (top), FeOOH rich sediments from Karginskiy interstadial (middle) and Fe sulfides in sediments corresponding to MIS 5a (bottom). The assignment of the reduction (negative) peaks: C1 $Mn^{III,IV}$ oxides, C2 ferrihydrite, C3 well crystalline Fe oxide (goethite), C4 Fe sulfide and the oxidation (positive) peak: A1 Fe sulfide. Arrows indicate the beginning and direction of the polarization.

however the corresponding local maxima were also used for obtaining the primary date points (Fig. 3). The remaining samples were dated by a linear interpolation between the tie points. The resulting mean sedimentation rate in core VER98-1-13 is 4.2 cm/ky, which is in good agreement with previously published data (Peck et al., 1994; Oda et al., 2002; Kravchinsky et al., 2003; Demory et al., 2005a).

3.2. Voltammetry of microparticles (VMP)

VMP is specific to Fe-oxides and sulfides with a detection limit of about ~0.1%. The sensitivity is an order of magnitude better than that for XRD (Grygar and van Oorschot, 2002). The method is not commonly used for sediment analysis but has been verified by an inter-laboratory trial (Grygar et al., 2002) and through comparisons with other techniques (Grygar et al., 2003). VMP is not a quantitative analytical method but is suitable for identification (Fig. 4).

In the top part of the sediment, namely at depths of 8–13 cm (up to 2 ky BP), $Mn^{III,IV}$ oxides (reduction at E_P+0.45 V vs. SCE) and ferrihydrite (reduction peak potential E_P between −0.15 to −0.22 V vs. SCE) are common. Both these oxides are responsible for striking reddish brown color at the core top (Fig. 2). The minor voltammetric peak of ferrihydrite were obvious down to a depth of 45 cm (16 ky BP), i.e. below the diatomaceous layers of the Holocene. In samples from greater depths VMP peaks of $Mn^{III,IV}$ oxides and ferrihydrite were not found.

In all samples from the last glacial maximum (MIS 2) and from MIS 3 well crystalline goethite was identified according to its reduction peak at E_P −0.75 V vs. SCE

Table 1
Mean position (standard deviations in parentheses), mean widths (FWHM) and assignment of the Gaussian absorption bands in the diffuse reflectance spectra of the entire series (133 spectra, 0–5.7 m, 0–132 ky BP)

Band	Center [cm^{-1}]	FWHM [cm^{-1}]	Band assignment	Possible minerals
A	10985 (54)	1930	Octahedral Fe^{III}	All Fe^{III} oxides and silicates
B	13929 (100)	2613	Fe^{II}–Fe^{III}	Biotite, chlorite
C	15984 (177)	2613	Octahedral Fe^{III}	All Fe^{III} oxides and silicates
D	18499 (233)	2648	Magnetically coupled octahedral Fe^{III}–Fe^{III}	Hematite
E	20473 (220)	2650	Magnetically coupled octahedral Fe^{III}–Fe^{III}	FeOOH
F	23635 (318)	2676	Octahedral Fe^{III}	Goethite
G	29000 (fixed)	11876	Octahedral Fe^{III}	All Fe^{III} oxides

The bands were assigned according to Sherman (1985, 1987), Barrón and Torrent (1986), Deaton and Balsam (1991), and Hradil et al. (2004).

(Grygar et al., 2002; Grygar and van Oorschot, 2002). After heating to 320 °C goethite was converted to protohematite with E_P shifting to a more positive value of −0.45 V vs. SCE while the peak of the minor hematite component remained at E_P −0.75 V vs. SCE. This test is suitable to distinguish between these two phases (Grygar and van Oorschot, 2002). According to this test goethite was approximately ten times more abundant than hematite. The goethite concentration was substantially lower in samples from greater depths and traces of goethite were only found in the interval corresponding to MIS 5d.

In some samples voltammetry revealed Fe sulfide admixtures (oxidation peak at +0.75 V vs. SCE and a well-defined reduction peak at −0.85 V vs. SCE, the latter is not shown in Fig. 4). A smaller amount of Fe sulfides were found in two samples from the middle of MIS 5a and in many samples from the climatic transition from MIS 6 to MIS 5e while the largest Fe-sulfide accumulation was found in sediments from the middle of the last interglacial (samples with an absolute minimum in the MS record). This highlights that reductive transformation of ferric oxides occurs as result of high bioproductivity in the lake.

3.3. Diffuse reflectance spectroscopy (DRS)

According to powder XRD analyses and findings from mineralogical studies (Grachev et al., 1998; Horiuchi et al., 2000; Fagel et al., 2003; Grygar et al., 2005), the main coloring agents of Lake Baikal's sediments are amphiboles, dark micas (biotite), chlorite or chloritized biotite, and FeOOH. This mineral assemblage matches well with the absorbing groups included in Table 1. Diffuse reflectance spectra, their 2nd derivatives with their minima corresponding to the absorption maxima and an example of spectral deconvolution are shown in Fig. 5.

The absorption bands A, B, and C are common to several Fe-bearing silicates (Hradil et al., 2004). Band B is due to a Fe^{II}–Fe^{III} pair e.g. as may occur in dark micas. Hypothetically, it could also be due to other ferrous compounds such as Fe-phosphate (vivianite) but the latter phase was not detected by XRD (detection limit is ~1 wt.%) and in X-ray fluorescence analysis the total P content in samples is <0.1% (except for the redox front at the top of the profile where ~0.2% P is bonded to Fe oxides). The bands D and E can be attributed to relatively intense d–d electron-pair transitions (EPT) of hematite and FeOOH (Sherman, 1985). Although the term FeOOH could include both common polymorphs of FeOOH (α- and γ-FeOOH) and ferrihydrite according to the EPT-band position, VMP identified

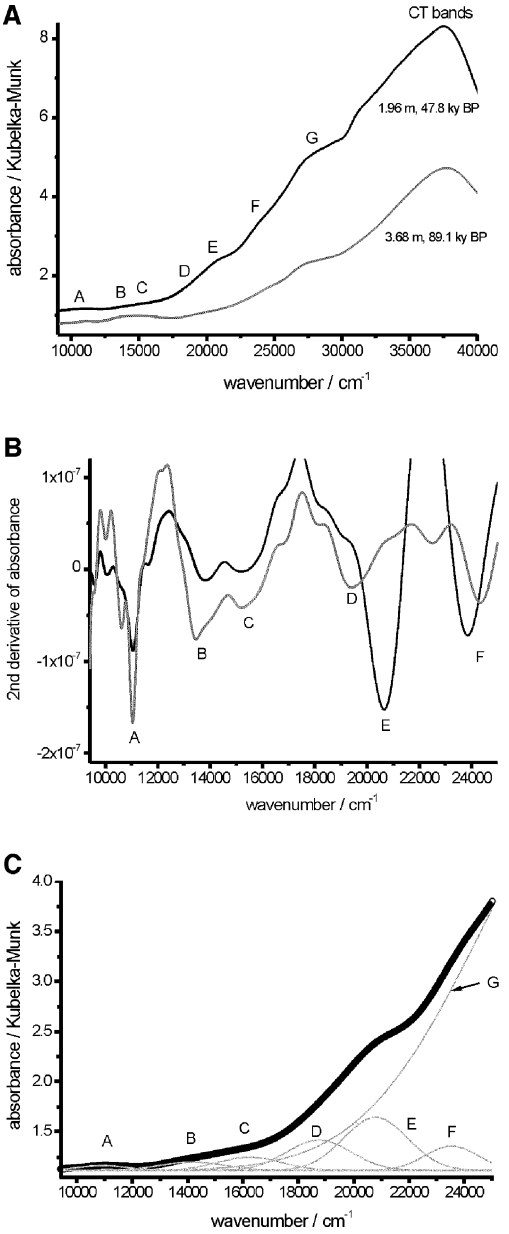

Fig. 5. Diffuse reflectance spectra. Smoothed diffuse reflectance spectra of two samples with their depths and corresponding ages (A), their second derivative (B) and the spectral deconvolution (C, circles: data points, thick line: fitted spectra, thin lines: Gaussian components). The band denotation (A–G) is the same as in Table 1.

goethite as a major Fe^{III} oxide and a ferrihydrite admixture only at the top of the profile. Importantly, Fe^{III} oxides also contribute to the bands A and C. This overlap means that one cannot interpret the DRS data in terms of percentages of the mineral composition. In the deconvolution the band G was fixed at 29 000 cm^{-1}; its ascending part represents the "background" in the Vis-region due to a much stronger absorption of Fe^{III}

oxides and oxidic species in near UV. Hence, the resulting color of the sediment is attributable to several coloring agents: goethite α-FeOOH (yellowish or brownish hues), ferrihydrite (reddish hue), $Mn^{III,IV}$ oxides (dark hues), and $Fe^{II,III}$ silicates (greenish hues). The resulting color is in line with the lithological description in Fig. 2. The poorly pronounced color of the sediments indicates a considerable overlap of the absorption bands. It is worthwhile mentioning that not all Fe-bearing minerals can be visualized by DRS. For example the Fe sulfide revealed in some samples by VMP has no definite absorption bands in the visible-near IR region.

Fe-bearing minerals are probably the main mineral coloring agent in the sediment. Organic matter and Fe sulfide(s) can only increase the absorption background (greyness) of the reflectance spectra and hence cannot affect the spectral deconvolution. The mean Ti (~0.5%) and Mn (<0.1%) contents are one and two orders of magnitude, respectively lower than that for Fe (3–6%) except for the redox front where the Mn content is higher (~1%). In that brown layer $Mn^{III,IV}$ oxides identified by VMP contribute to the color. The color of the fresh sediments documented by the lithological description (Fig. 2) was the same as the color of the dry powders used for DRS, hence there was no reason to assume the presence of air-sensitive pigments in the original sediments.

3.4. DRS-based proxies

The area of band B is proportional to the amount of Fe^{II}–Fe^{III} pairs in Fe-bearing alumosilicates. Band C is composed of Fe^{III} in silicates and oxides and hence the ratio of the areas of bands B and C, denoted further as B/C, is a proxy of Fe^{II}/Fe^{III} ratio in the mineral assemblage. In sediments with low Fe oxides content B/C mostly reflects Fe^{II}/Fe^{III} ratio in alumosilicates (Fig. 6). In sediments with substantially increased FeOOH (band E) the B/C ratio is systematically decreased. We processed DRS of synthetic goethite diluted to 5% by calcite and found that the ratio of the areas of bands C and E is 0.11. In Fig. 7 we hence plotted ratio B/(C-0.11·E) to permit independent data interpretation of the highly varying FeOOH content in sediments younger than 75 ky BP.

3.5. Diatom analysis

Diatom counts were made on sediments from 120 to 60 ky BP to characterize the cooling during the last interglacial (MIS 5). Total diatom concentrations provide an overall indicator of productivity within Lake Baikal while species/genera concentrations can provide more season specific information. In the analyzed samples three dominant taxonomic groups were identified; *Aulacoseira* sp., almost entirely comprised of *Aulacoseira baicalensis* (Meyer) Simonsen and *Aulacoseira skvortzowii* (Edlund, Stoermer and Taylor), *Cyclotella sp*. dominated by *Cyclotella baicalensis* (Meyer) Skv., *Cyclotella minuta* (Skv.) Antipova, and *Cyclotella ornata* (Skv.) Flower and *Stephanodiscus sp*., dominated by the large *Stephanodiscus grandis* (Khursevich and Loginova).

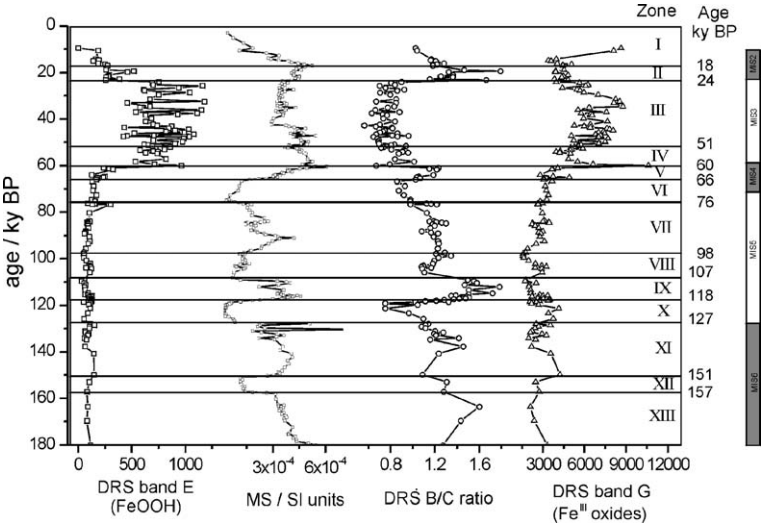

Fig. 6. Thirteen zones distinguished by MS and DRS-based proxies between 180 and 7 ky BP. The Holocene (the uppermost part) cannot be evaluated because of the presence of an actual redox front making DRS inapplicable.

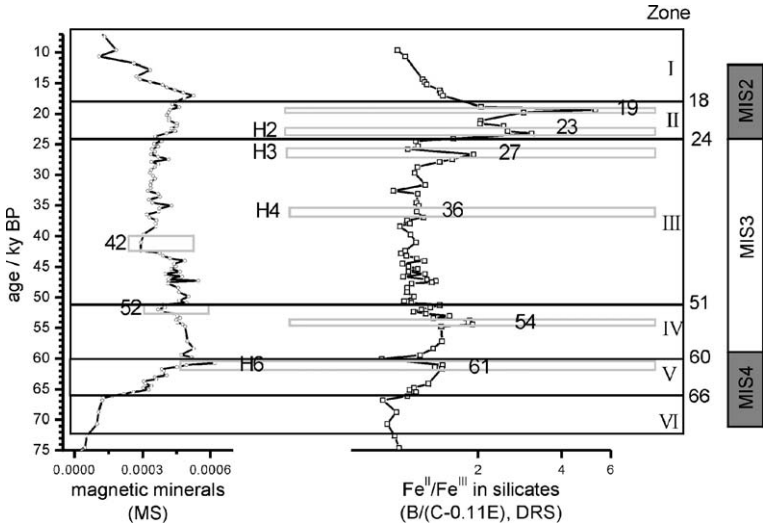

Fig. 7. Seven zones identified between 75 and 7 ky BP and the present, i.e. late part of the last glacial cycle with conventional dating. The position of local millennial extremes (MS minima and B/(C-0.11 · E) maxima) with their dating is indicated by grey rectangles. The stratigraphic position of Heinrich events (Cortijo et al., 1995) are marked by H#.

A. baicalensis blooms under the ice in spring with a temperature optima of c. 3 °C with higher concentrations often related to extended ice-free periods and/or clear ice conditions or ice with a snow depth of less than 10 cm (Bradbury et al., 1994; Jewson and Granin, 2000; Richardson et al., 2000). Similarly, *A. skvortzowii* blooms in spring also being a colder water taxa with a temperature optima of less than 5 °C (Morley, 2005). *C. baicalensis*, *C. minuta*, and *C. ornata* all have similar ecologies but occupy different temporal distributions within the lake (Morley, 2005). While *C. baicalensis* and *C. ornata* generally peak during the spring diatom bloom and *C. minuta* in the autumn bloom, all three species are often present in the surface waters throughout the year particularly during the autumn months following the end of summer stratification (Morley, 2005). Compared to the aforementioned *Aulacoseira* sp., all three Cyclotella taxa have a much higher tolerance and optima to warmer water conditions (Bradbury et al., 1994; Morley, 2005). As such, overall increased concentrations of *Cyclotella* sp. can here be related to year round warmer, more favorable, conditions and a reduced annual ice cover duration.

The correlation between the inorganic and diatom-based proxies is displayed in Fig. 8. Prior to 109 ky BP few diatom frustules are present in the sediment indi-

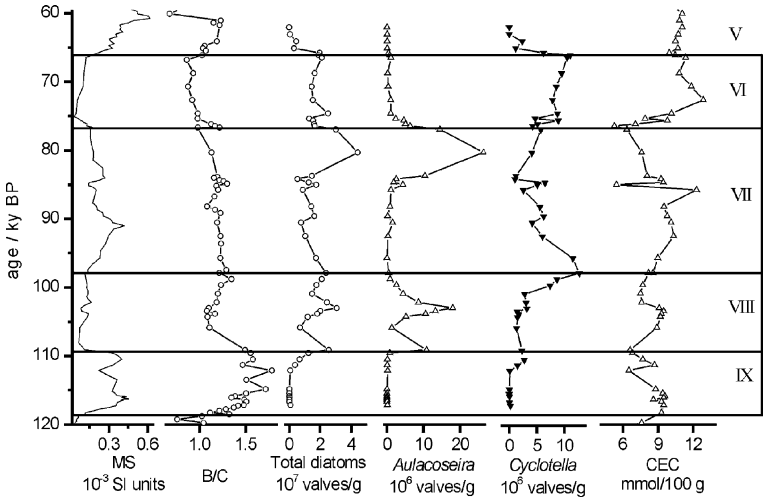

Fig. 8. MS, B/C ratio from DRS, total diatom concentration, concentration of *Aulacoseira* and *Cyclotella* sp. and cation exchange capacity (Grygar et al., 2005) during the climatic deterioration after the last interglacial.

cating a colder climate. This is in agreement with higher values of MS and B/C. After 109 kyr MS and B/C both decrease while total diatom concentrations and in particular *Aulacoseira* concentrations increase, reflecting a shift to warmer climatic conditions more favorable to large diatom blooms. *Aulacoseira* concentrations shows three maxima between 120–60 ky BP at c. 109 ky BP, c. 102 ky BP (MIS5c) and 84–77 ky BP which indicate warmer spring conditions, reduced seasonal ice cover and significant spring lake productivity. Conversely, the *Cyclotella* record is marked by high concentrations from 100–96 ky and from 80–66 ky BP with the latter peak marking the transition from MIS 5 to the full glacial state of MIS 4. An overall increase in *Cyclotella* concentrations from 80–66 ky BP together with higher *Aulacoseira* concentrations from 84 to 77 ky BP therefore indicates an interval of warmer conditions and reduced annual ice cover towards the end of MIS 5. The dominance of *Cyclotella* taxa after the decline in *Aulacoseira* species reflects an increase in autumnal productivity relative to the spring bloom. A similar "replacement" of *A. baicalensis* by *Cyclotella* taxa at the end of MIS 5 is also found by Edlund and Stoermer (2000) in the south Basin of Lake Baikal indicating that this feature does not reflect local paleoconditions at site VER98-1-13. At c. 80 ky BP the pronounced Northern Hemisphere differences between summer and winter insolation, which characterized the last interglacial (MIS 5e), are replaced by a 10 ky period of warmer winters and colder summers relative to the present time (Berger, 1978). Such changes may have initiated changes in the water column leading to the increased relative importance of the autumn bloom over the spring bloom by preventing large populations of *Aulacoseira* sp. The end of the *Cyclotella* maximum is followed at 65 ky BP by a substantial decrease in all diatom concentrations which coincides with changes in B/C and MS to indicate a period of dramatic cooling. Following this few diatom valves remain in the sediment with the establishment of full glacial conditions and extended ice cover over the lake preventing significant diatom blooms while B/C and MS both remain high.

4. Discussion

The general pattern of the MS record (Figs. 2, 6, and 7) agrees with the general pattern of low MS during warm/humid climates found by Peck et al. (1994) and Demory et al. (2005a). The MS minima at 126–119, 109–97, 76–66 ky BP and above 11 ky BP correspond roughly to MIS 5e, 5c, 5a and the Holocene, respectively. These periods also corresponds to the largest concentration of biogenic silica according to Edlund and Stoermer (2000), Prokopenko et al. (2001b), Prokopenko and Williams (2003), and Chebykin et al. (2004). The most probable reason for the decreased MS in warmer periods is the increased influx of organic matter to the sediment, causing the reductive dissolution of magnetite or its conversion to sulfides. Hence, the MS record is sensitive to the main climatic stages. The relationship between MS and diatom concentration was verified in the time interval between 120 and 60 ky BP (Fig. 8). MS is therefore a very good climatic proxy that can be obtained at high temporal resolution with much less time-consuming work than, for example, diatom analysis.

4.1. Clay mineral record

Analysis of expandable clay minerals in core VER98-1-13 (Grygar et al., 2005) revealed one unexpected feature: the total amount of these minerals, expressed as the total cation-exchange capacity (CEC), was least in the warmest periods between 130 and 60 ky BP (MIS 5e, MIS 5c, and MIS 5a) and increased in the cold stages (MIS5 d, MIS 4) and particularly between 60 and 24 ky BP (moderate stage MIS 3). This pattern means that the expandable clay minerals (smectite or vermiculite and illite–smectite) were more abundant in the periods limiting or even excluding their neoformation. Chebykin et al. (2004) also found an increased absolute influx of clay material in cold periods and related this to the erosion of river valley Quaternary deposits by local glaciers. Another explanation could be a change in transport mechanisms from fluvial in more humid periods to eolian in drier periods (Grygar et al., 2005).

The diatom record was obtained to answer two principal questions; whether the CEC record is independent of diatom abundance and what could cause the different timings in the changes of inorganic proxies between 76 and 60 ky BP (cooling MIS 5/MIS 4, Fig. 7). As follows from Fig. 8, the diatom record revealed two principal changes. The first is a "replacement" of the cold-water diatoms *Aulacoseira* sp. by the warmer-water *Cyclotella* sp. at 77 ky BP. A similar change in the diatom genera at the end of the warm period (MIS 5) was also reported by Edlund and Stoermer (2000) and Chebykin et al. (2004). This change coincides with an increase in the content of expandable clay minerals, expressed as CEC of the sediment, at 77 ky BP (Fig. 8, Grygar et al., 2005). The total concentration of diatoms remained relatively high until the second major change

at 66 ky BP when diatoms vanished from the sediment at the onset of a very cold stage. This coincides with the sharp increase in MS. The environmental conditions between 77 and 66 ky BP were therefore different with respect to both the warm/humid interglacial (MIS 5e) and cold/dry (MIS 4) periods.

In the period of small MS variations between 66 and 18 ky BP there are several striking features in the DRS derived proxies. One of them is the substantially increased content of FeOOH in the sediments from 59 to 23 ky BP, corresponding roughly to MIS 3. There are two well-defined maxima in B/C or B/(C-0.11·E) corresponding to the coldest stages of MIS 5d, MIS 4, and MIS 2 and lasting 11, 6, and 6 ky, respectively. The B/C ratio is a proxy of the redox state of Fe in silicates and oxides and it is known that the redox state of Fe is a measure of the weathering of primary minerals during pedogenesis (Adamová et al., 2002). We can hence attribute the high B/C values to an enhanced detrital input of less intensively chemically weathered material, i.e. with a lower mean Fe valence. The species with neighboring Fe^{II}–Fe^{III} ions responsible for band B is most probably present in Fe-bearing chlorites and black micas, which are unstable under humid and oxic conditions.

4.2. Climatic evolution during the past 160 ky

Based on MS and DRS records, diatom analysis and clay mineral abundance (the last taken from Grygar et al., 2005) we have identified 13 Zones characterising different environmental conditions between 180 and 7 ky BP (Roman numerals in Figs. 6 and 7). Zone boundaries are mostly based on changes recorded in more than one proxy. Repeatedly the total Fe oxidic species (band G) increased at the zone boundaries (Fig. 6). During cooler intervals Fe^{II}/Fe^{III} in silicates (B/C or B/(C-0.11·E)) show significant peaks. We hence explain increasing B/C or B/(C-0.11·E) as higher fluxes of less weathered mineral detritus into Lake Baikal. Part of this physically weathered material was probably transported by ephemeral local glaciers accumulating on mountains adjacent to the lake.

MS and B/C values indicate cold conditions before 157 ky BP (Zone XIII; lower MIS 6) and during the lower part of Zone XI (151–127 ky BP), both corresponding to the Taz glacial (MIS 6). From 157–151 ky BP (Zone XII) a slight warming, representing an interstadial of MIS 6, is recorded at a time when insolation increased in the high latitudes of the Northern Hemisphere (Berger, 1978). This is evidenced by lowered MS values and B/C ratios.

Termination II is expressed in three distinct MS oscillations approximately dated to 133, 130, and 128 ky BP (at the top of Zone XI) which can be related to fine laminae with abundant diatoms starting approximately at 138 ky BP. (Fig. 2). Moreover around 137 ky BP, superimposed on generally decreasing MS values, the B/C ratio decreased and concentration of Fe^{III} oxides increased to values similar to those observed in the Kazantsevo Interglacial. Altogether this points to a stepwise increase in chemical weathering in the watershed and a temporarily enhanced lacustrine bioproductivity. Voltammetry data reveals the highest Fe sulfide accumulations at this time. Watanabe et al. (2003) observed sharp peaks of S concentration at each important climatic transition including Termination II (MIS6/MIS5e) which were explained by strongly fluctuating sedimentation rates and the freezing of the paleoredox front (Demory et al. (2005b). The warming during Termination II, from approximately 135 to 128 ky BP, was therefore accompanied not only by dramatic environmental fluctuations in the watershed but also by fluctuations in the water body.

During the Kazantsevo interglacial (Zone X, 127–118 ky BP) chemical weathering was at a maximum in the watershed (lowest B/C) and lake bioproductivity was highest (lowest MS). Ferrimagnetic minerals are in very low concentrations whereas the content of total Fe^{III} oxides is slightly elevated. Part of this Fe is present in sulfides indicating increased reducing conditions in the sediments. The dating of Zone X is in perfect agreement with another dated from Continent Ridge (Demory et al., 2005a) where Roiual and Mackay (2005) and Granoszewski et al. (2005) dated diatom and pollen optimum conditions to 128–117 ky BP.

Between 118–109 ky BP (Zone IX) the pronounced local maxima of MS and B/C ratios again indicate an increased influx of less weathered primary minerals to the sediment. This interval (MIS 5d) together with the last glacial maximum (Zone 2; MIS 2) clearly documents a period containing the least intensive chemical weathering during the last 150 ky. However, several fluctuations with local maxima of B/C and MS (rusty layer at 116–115 ky BP; probably an accumulation of Fe^{III} oxides) might correspond to periods of short climatic warming. At the top of Zone IX a MS oscillation with a maximum at 110 ky BP resembles the oscillations at the top of Zone XI at the MIS 6/MIS 5e transition. The fluctuations might be time equivalent to the Dansgaard–Oeschger events 25 and 26 recorded in the North Greenland ice core record (North Greenland Ice Core Project members, 2004). Only shortly later a subsequent amelioration occurred at the top of

the Zone when *Stephanodiscus grandis* together with *Aulacoseira* sp. and *Cyclotella* sp. become abundant.

Between 109–98 ky BP (Zone VIII), MS is almost as low as in Zone X (the Kazantsevo Interglacial). Total contents of Fe oxides are elevated and the B/C ratio is at a local minimum in the lower part of the Zone, indicating an elevated discharge of organic matter and chemically weathered detritus into the lake. Bioproductivity is also increased as shown by high diatom concentrations. The MS variation and a CEC maximum at 103 ky BP (Grygar et al., 2005) were attributed to a middle MIS 5c cooling described earlier by Prokopenko et al. (2001a). The distinct maximum of the cold-water diatom *Aulacoseira* sp. may help to delineate that this cooling might only have been seasonal and thus only have affected the late winter and spring lake conditions (Fig. 8).

MS and B/C values in Zone VII (98–76 ky BP) are between values typical of the warmest and coldest periods of MIS 5. Steadily decreasing diatom concentrations between 93 and 84 ky BP correspond to increased MS values as also reported earlier by Chebykin et al. (2004). In the VER98-1-13 record two cold minima at about 90 ky BP (diatom concentration minimum and a distinct MS maximum) and at 85–83 ky BP (weak B/C maximum, MS maximum and diatom concentration minimum) are probably related to abrupt climatic changes which are also observed in the North Greenland ice core (North Greenland Ice Core Project members, 2004). An interesting feature of the DRS-based proxies in Zone VII is their continuous shift towards values that will prevail in Zone III, corresponding to MIS3. Before the end of Zone VII the cold-water *Aulacoseira* sp. shows a maximum abundance indicating reduced snow/ice covering on the ice on the lake and hence relatively warmer conditions in Central Siberia. Zone VII ends with a sharp B/C maximum and a diatom minimum at about 76 ky BP (Fig. 8). This date matches closely to North Atlantic Heinrich event 7, dated to ~75 ky BP, and possibly coincides with the top of the diatomaceous layers observed elsewhere at the Academician Ridge (Prokopenko et al., 2001b; Chebykin et al., 2004) and at the Selenga Delta (Prokopenko et al., 2001a).

Zone VI (76–66 ky BP) represents an intermediate stage between late MIS 5a and MIS 4. Both low B/C and MS records are very similar to the values recorded during the warmest part of the Kazantsevo interglacial reflecting an increased discharge of highly weathered detrital minerals and organic matter to the lake. Interestingly, the concentration of diatom frustules remained rather high in VER98-1-13 though the diatom assemblages shows a characteristic change between 76 and 75 ky BP with *Aulacoseira* sp. replaced by the warmer-water genera *Cyclotella* sp. MS values remain low, as if lake bioproductivity was maintained during this period and/or the influx of terrigenous organic materials continued uninterrupted. According to Watanabe et al. (2003) the anoxic conditions in the sediment and the terrestrial origin of organic matter was even more important than the lake's primary bioproductivity. This is corroborated by the observation that fluvial input increased in this period. Prokopenko et al. (2001a) observed more terrigenous material in the Selenga Delta sediments at ~70 ky BP. Its peak was attributed to changes related to Heinrich Event 6. Between 76 and 72 ky BP the total amount of expandable clay minerals in the sediment also increased significantly (Fig. 8), indicating that it could be related to a change in the sediment source area or transport mechanism (Chebykin et al., 2004; Grygar et al., 2005). Goldberg et al. (2005) proposed that a dramatic decrease in water inflow to the lake occurred approximately at 80 ky BP as a result of decreased and fluctuating level of rainfalls between 80 and 67 ky BP. Zone VI may hence be considered a transient period embedded between two colder periods with substantial environmental changes in the watershed but still relatively high lake bioproductivity.

A dramatic fall in total diatom concentration starts in Zone V (66–60 ky BP) and a simultaneous increase occurs in MS and B/C indicating that organic matter input ceased and the contribution of unweathered minerals increased. The significant accumulation of Fe^{III} oxides occurs at the boundaries of Zones VI/V (DRS band G, Fig. 6). Again a prominent MS peak and a B/C maximum is observed at 61 ky BP. The cold/arid climatic condition in Zone V corresponds to the extremely cold conditions reported elsewhere from 67.4–61.2 ky BP, for example from a terrestrial record in South France (Genty et al., 2003). Unlike the MIS 4 signals in SPECMAP, this period was very cold in Central Siberia.

In the last glacial cycle FeOOH peaks between 60–51 ky BP (Zone IV) and, surprisingly, the FeOOH content remains high through Zone II which corresponds to MIS3. In this interval, which was supposed to be cold and dry in this part of Siberia, the Baikal watershed was probably covered with permafrost (Chlachula, 2001). FeOOH, especially highly crystalline goethite as observed by voltammetry, can only form under humid conditions by chemical weathering in the watershed. We propose that the sediment source changed rather than the neoformation FeOOH. This matches well with a high influx of expandable clay

minerals during this period (Grygar et al., 2005, Fig. 8). The presence of FeOOH requires that the B/C ratio be corrected to serve as an estimate of Fe^{II}/Fe^{III} in silicates since FeOOH contributes to band C. The value of B/(C-0.11·E) was hence plotted in Fig. 7.

An environmental oscillation is obvious between a local maximum of B/(C-0.11·E) at 54 ky BP and a local minimum in MS at 52 ky BP (Fig. 7). The distinct maximum of B/(C-0.11·E) is very similar to the maxima observed in Zones V, III, and II, which can likely be attributed to Heinrich events. However, the dating of H5 is uncertain (Cortijo et al., 1995); meaning the signal may instead represent a series of local cooling events that occurred between 60 and 40 ky BP. However, the short-lasting MS minimum at 51 ky BP coincides with a sudden, short lived, increase in diatom concentrations found by Swann et al. (2005) at Continent Ridge.

Zone III (51–24 ky BP), corresponding to the Karginskiy interstadial (MIS 3), is characterised by a high FeOOH content with MS almost increasingly to values previously reached during the extremely cold stage of Zone IX (MIS 5d). This is in agreement with Swann et al. (2005) who assumed that the short diatom boom at 51 ky BP was ended by a sudden climatic deterioration at ~50 ky BP. A further MS minimum at 42 ky BP is probably related to an increase in lake productivity during the Karginskiy Interstadial climatic optimum, which has previously been recorded in diatom concentration by Prokopenko et al. (2001a), Chebykin et al. (2004), and Swann et al. (2005) between approximately 50 and 35 ky BP, i.e. between Heinrich events 5 and 4, respectively. Fe^{II}/Fe^{III} in silicates has a rather stable value in Zone III except for two maxima in the upper part of the Zone: a less pronounced one at 36 ky BP and a sharp one at 27 ky BP. Both maxima are simultaneous (within about 1 ky) with a slight MS variations at 35 and 27 ky BP. These can be attributed to Heinrich events 4 and 3, respectively.

From 24–18 ky BP (Zone II), representing the last glacial maximum (Sartan glaciation, early part of MIS 2), maximal values of B/(C-0.11·E) and a drop in FeOOH content occur. Furthermore, there are two distinct peaks in B/(C-0.11·E) (23 and 19 ky BP) coinciding with clearly visible MS spikes. The earlier one (23 ky BP) can possibly be related to Heinrich event 2. Termination I is well expressed: the MS values of Zone I (after 18 ky BP) remain in a range comparable to the end of Zone II up to about 15 ky BP, although after 17 ky BP the MS value systematically decrease. At the top of the core DRS applicability is severely limited due to the proximity of the redox front, a brown layer in the upper part of the sediments. Both ferrihydrite and $Mn^{III,IV}$ oxides present here makes the spectra almost featureless with blurred absorption bands in the Vis part of the spectra.

5. Conclusions

MS and DRS-based sediment proxies from core VER98-1-13 enabled the reconstruction of the main climatic stages and permitted the comparison of them to the marine oxygen isotope stages. The climate-independent age model permitted us to identify several differences between the marine isotope and Baikal climatic stages. The cooling that finished the last interglacial proceeded to a stage between 76 and 66 ky BP with an environment that probably was drier than the preceding period but still much warmer than the subsequent cold extreme between 66 and 60 ky BP. The MS record indicates sub-Milankovitch warming events related to a temporary increase in lake bioproductivity while DRS records revealed numerous sub-Milankovitch events in the last glacial cycle, lasting about 1–2 ky, typified by an influx of chemically less weathered minerals. The observed events coincided with Heinrich events, Greenland stadials and/or Dansgard–Oeschger events, i.e. changes in the North Atlantic region. Some of these sharp changes coincided with the "switching" between climatic stages during the last 100 ky. From the mineral records it is obvious that that switching was rather fast, lasting 1–2 ky in the case of coolings, and 1–5 ky in the case of warmings. Substantial warming transitions, preceded by environmental oscillations (at 133–128 ky BP, about 110 ky BP and about 13 ky BP), were revealed by MS maxima and by accumulations of Fe sulfides and/or Fe^{III} oxides. Substantially increased concentrations of FeOOH, most likely goethite, were also found in sediments deposited between 60 and 24 ky BP. The reasons for this are not clear but one possible explanation is an enhancement in eolian input of Tertiary weathering crusts to the lake. This probably also relates to the input of expandable clay minerals in periods of low intensity chemical weathering.

Acknowledgements

The authors thank several institutions for funding the sampling, measuring and interpretation. Coring and core storage was funded by GFZ Potsdam, Germany. The sampling and magnetic measurements were supported by CONTINENT Project (EC Project EVK 2-2000-00057). XRD and spectral analyses were funded by the Ministry of Education of CR (LN00A028) and

the Grant Agency of the Czech Republic (A3032401). XRF analyses were kindly provided by David Kolousek, Institute of Chemical Technology in Prague, Czech Republic. The authors are grateful to N. Nowaczyk and F. Demory (GFZ Potsdam, Germany) for important discussions relating to the magnetic measurements and the age model.

References

Adamová, M., Havlíček, P., Šibrava, V., 2002. Mineralogy and geochemistry of loesses in southern Moravia. Bull. Czech Geol. Survey 77, 29–41.

Almeida, C.M.V.B., Giannetti, B.F., 2003. The electrochemical behavior of pyrite–pyrrhotite mixtures. J. Electroanal. Chem. 553, 27–34.

Bakardjieva, S., Bezdička, P., Grygar, T., Vorm, P., 2000. Reductive dissolution of microparticulate Mn oxides. J. Solid State Electrochem. 4, 306–313.

Balsam, W.L., Beeson, J.P., 2003. Sea-floor sediment distribution in the Gulf of Mexico. Deep-Sea Res. I 50, 1421–1444.

Balsam, W.L., Otto-Bliesner, B.L., Deaton, B.C., 1995. Modern and last glacial maximum eolian sedimentation patterns in the Atlantic Ocean interpreted from sediment iron oxide content. Paleoceanography 10, 493–507.

Bangs, M., Battarbee, R.W., Flower, R.J., Jewson, D., Lees, J.A., Sturm, M., Vologina, E.G., Mackay, A.W., 2000. Climate change in Lake Baikal: diatom evidence in an area of continuous sedimentation. Int. J. Earth Sci. 89, 251–259.

Barrón, V., Torrent, J., 1986. Use of the Kubelka–Munk theory to study the influence of iron oxides on soil colour. J. Soil Sci. 37, 499–510.

Battarbee, R.W., Kneen, M.J., 1982. The use of electronically counted microspheres in absolute diatom analysis. Limnol. Oceanogr. 27, 184–188.

Berger, A.L., 1978. Long-term variations of caloric insolation resulting from the Earth's orbital elements. Quat. Res. 9, 139–167.

Bradbury, J.P., Bezrukova, Y.V., Chernayaeva, G.P., Coleman, S.M., Khursevich, G., King, J.W., Likhoshway, Y.V., 1994. A synthesis of post-glacial diatom records from Lake Baikal. J. Paleolimnol. 10, 213–252.

Channell, J.E.T., 1999. Geomagnetic paleointensity and directional secular variation at Ocean Drilling Program (ODP) site 984 (Bjorn Drift) since 500 ka: comparisons with ODP site 983 (Gardar drift). J. Geophys. Res., B: Solid Earth 104, 22,937–22,951.

Chebykin, E.P., Edgington, D.N., Goldberg, E.L., Phedorin, M.A., Kulikova, N.S., Zheleznyakova, T.O., Vorob'yova, S.S., Khlystov, O.M., Levina, O.V., Ziborova, G.A., Grachev, M.A., 2004. Uranium-series isotopes as proxies of Late Pleistocene climate and geochronometers in bottom sediments of Lake Baikal. Geol. Geofiz. 45, 539–556.

Chlachula, J., 2001. Pleistocene climate change, natural environments and paleolithic occupation of the Angara–Baikal area, east Central Siberia. Quat. Int. 80–81, 69–92.

Cortijo, E., Yiou, P., Labeyrie, L., Cremer, M., 1995. Sedimentary record of rapid climatic variability in the North Atlantic Ocean during the last glacial cycle. Paleoceanography 10, 911–926.

Deaton, B.C., Balsam, W.L., 1991. Visible spectroscopy — a rapid method for determining hematite and goethite concentration in geological materials. J. Sediment. Petrol. 61, 628–632.

Demory, F., Nowaczyk, N.R., Witt, A., Oberhänsli, H., 2005a. High-resolution magnetostratigraphy of Late Quaternary sediments from Lake Baikal, Siberia: timing of intracontinental paleoclimatic responses. Glob. Planet. Change 46, 167–186.

Demory, F., Oberhänsli, H., Nowaczyk, N.R., Gottschalk, M., Wirth, R., Neumann, R., 2005b. Detrital input and early diagenesis in sediments from Lake Baikal revealed by rock magnetism. Glob. Planet. Change 46, 145–166.

Edlund, M.B., Stoermer, E.F., 2000. A 200,000-year, high-resolution record of diatom productivity and community makeup from Lake Baikal shows high correspondence to the marine oxygen-isotope record of climate change. Limnol. Oceanogr. 45, 948–962.

Fagel, N., Boski, T., Likhoshway, L., Oberhansli, H., 2003. Late Quaternary clay mineral record in Central Siberia Lake Baikal (Academician Ridge, Siberia). Palaeogeogr. Palaeoclimatol. Palaeoecol. 193, 159–179.

Goldberg, E.L., Chebykin, E.P., Vorobyova, S.S., Grachev, M.A., 2005. Uranium signals of paleoclimate humidity recorded in sediments of Lake Baikal. Dokl. Earth Sci. 400, 52–56.

Grachev, M.A., Vorobyova, S.S., Likhoshway, Y.V., Goldberg, E.L., Zbirova, G.A., Levina, O.V., Khlystov, O.M., 1998. A high-resolution diatom record of the palaeoclimates of East Siberia for the last 2.5 My from Lake Baikal. Quat. Sci. Rev. 17, 1101–1106.

Granoszewski, W., Demske, D., Nita, M., Heumann, G., Andreev, A.A., 2005. Vegetation and climate variability during the Last Interglacial evidenced in the pollen record from Lake Baikal. Glob. Planet. Change 46, 187–198.

Genty, D., Blamart, D., Ouahdi, R., Gilmour, M., Baker, A., Jouzel, J., Van-Exter, S., 2003. Precise dating of Dansgaard–Oescheger climate oscillations in Western Europe from stalagmite data. Nature 421, 833–837.

Grygar, T., Bezdička, P., Hradil, D., Doménech-Carbó, A., Marken, F., Pikna, L., Cepriá, G., 2002. Voltammetric analysis of Fe oxide pigments. Analyst 127, 1100–1107.

Grygar, T., van Oorschot, I.H.M., 2002. Voltammetric identification of pedogenic iron oxides in paleosol and loess. Electroanalysis 14, 339–344.

Grygar, T., Dědeček, J., Kruiver, P., Dekkers, M.J., Bezdička, P., Schneeweiss, O., 2003. Iron Oxide Mineralogy in Late Miocene Red Beds from La Gloria, Spain: rock-magnetic, voltammetric and VIS spectroscopy analyses. Catena 53, 115–132.

Grygar, T., Bezdička, P., Hradil, D., Hrušková, M., Novotná, K., Kadlec, J., Pruner, P., Oberhänsli, H., 2005. Characterization of expandable clay minerals in Lake Baikal sediments by thermal dehydration and cation exchange. Clays Clay Miner. 53, 389–400.

Helmke, J.P., Schulz, M., Bauch, H.A., 2002. Sediment-colour record from the Northeast Atlantic reversals patterns of millennial-scale climatic variability during the past 500,000 years. Quat. Res. 57, 49–57.

Horiuchi, K., Minoura, K., Hoshino, K., Oda, T., Nakamura, T., Kawai, T., 2000. Palaeoenvironmental history of Lake Baikal during the last 23000 years. Palaeogeogr. Palaeoclimatol. Palaeoecol. 157, 95–108.

Hradil, D., Grygar, T., Hrušková, M., Bezdička, P., Lang, K., Schneeweiss, O., Chvátal, M., 2004. Green earth pigment from Kadan region, Czech Republic: use of rare Fe-rich smectite. Clays Clay Miner. 52, 767–778.

Jewson, D.H., Granin, N.G., 2000. How can present day studies of diatoms help in understanding past climatic change in Baikal? Terra Nostra 9, 29–33.

Kashiwaya, K., 2003. Long Continental Records from Lake Baikal. Springer-Verlag Tokyo. 370 pp.

Kravchinsky, V.A., Krainov, M.A., Evans, M.E., Peck, J.A., King, J.W., Kuzmin, M.I., Sakai, H., Kawai, T., Williams, D.F., 2003. Magnetic record of Lake Baikal sediments: chronological and paleoclimatic implication for the last 6.7 Myr. Palaeogeogr. Palaeoclimatol. Palaeoecol. 195, 281–298.

Mackay, A.W., Flower, R.J., Kuzmina, A.E., Granina, L.Z., Rose, N.L., Appleby, P.G., Boyle, J.F., Battarbee, R.W., 1998. Diatom succession trends in recent sediments from Lake Baikal and their relation to atmospheric pollution and to climate change. Philos. Trans. R. Soc. Lond., B Biol. Sci. 353, 1011–1055.

Mackay, A.W., Battarbee, R.W., Flower, R., Granin, N., Jewson, D.H., Ryves, D.B., Sturm, M., 2003. Assessing the potential for developing internal diatom-based transfer functions for Lake Baikal. Limnol. Oceanogr. 48, 1183–1192.

Morley, D.W., 2005. Reconstructing past climate variability in continental Eurasia. PhD Thesis, University College London, p. 388.

North Greenland Ice Core Project members, 2004. High-resolution record of northern hemisphere climate extending into the last interglacial period. Nature 431, 147–151.

Nowaczyk, N.R., Antonow, M., 1997. High-resolution magnetostratigraphy of four sediment cores from the Greenland Sea-I. Identification of the Mono Lake excursion, Laschamp and BiwaI/Jamaica geomagnetic polarity events. Geophys. J. Int. 131, 310–324.

Oda, H., Nakamura, K., Ikehara, K., Nakano, T., Nishimura, M., Khlystov, O., 2002. Paleomagnetic record from Academician Ridge, Lake Baikal: a reversal excursion at the base of marine isotope stage 6. Earth Planet. Sci. Lett. 202, 117–132.

Peck, J.A., King, J.W., Colman, S.M., Kravchinsky, V.A., 1994. A rock-magnetic record from Lake Baikal, Siberia: evidence for Late Quaternary climatic change. Earth Planet. Sci. Lett. 122, 221–238.

Prokopenko, A.A., Williams, D.F., 2003. Glacial/interglacial changes in the carbon cycle of Lake Baikal. In: Kashiwaya, K. (Ed.), Long Continental Records from Lake Baikal. Springer-Verlag Tokyo, pp. 163–185.

Prokopenko, A.A., Karabanov, E.B., Williams, D.F., Kuzmin, M.I., Khursevich, G.K., Gvozdkov, A.N., 2001a. The detailed record of climatic events during the past 75,000 yrs BP from the Lake Baikal drill core BDP-93-2. Quat. Int. 80–81, 59–68.

Prokopenko, A.A., Karabanov, E.B., Williams, D.F., Kuzmin, M.I., Shackleton, N.J., Crowhurst, S.J., Peck, J.A., Gvozdkov, A.N., King, J.W., 2001b. Biogenic silica record of Lake Baikal response to climatic forcing during the Brunhes. Quat. Res. 55, 123–132.

Pruner, P., Kadlec, J., Schnabl, P., Slechta, S., Chadima, M., 2004. Paleomagnetic and rock magnetic records from the Baikal Lake sediments. Geophys. Res. Abstracts, EGU, 6: 01518. ISSN: 1029-7006, Nice.

Richardson, T.L., Gibson, C.E., Heaney, S.I., 2000. Temperature growth and seasonal succession of phytoplankton in Lake Baikal, Siberia. Freshw. Biol. 44, 431–440.

Rioual, P., Mackay, A.W., 2005. A diatom record of centennial resolution for the Kazantsevo Interglacial stage in Lake Baikal, Siberia. Glob. Planet. Change 46, 199–219.

Ryves, D.B., Jewson, D.H., Sturm, M., Battarbee, R.W., Flower, R.J., Mackay, A.W., Granin, N.G., 2003. Limnol. Oceanogr. 48, 1643–1661.

Sherman, D.M., 1985. The electronic structures of Fe^{3+} coordination sites in iron oxides; applications to spectra, bonding, and magnetism. Phys. Chem. Miner. 12, 161–175.

Sherman, D.M., 1987. Molecular orbital (SCF-Xá-SW) theory of meta-metal charge transfer processes in minerals: I. Application to $Fe^{2+} \rightarrow Fe^{3+}$ charge transfer and "electron delocalization" in mixed-valence iron oxides and silicates. Phys. Chem. Miner. 14, 355–363.

Swann, G.E.A., Mackay, A.W., Leng, M.J., Demory, F., 2005. Climatic change in Central Asia during MIS3/2: a case study using biological responses from Lake Baikal. Glob. Planet. Change 46, 235–253.

Watanabe, T., Naraoka, H., Nishimura, M., Kinoshita, M., Kawai, T., 2003. Glacial-interglacial changes in organic carbon, nitrogen and sulfur accumulation in Lake Baikal sediment over the past 250 kyr. Geochem. J. 37, 493–502.